

of the logarithm of ageing time. The method of calculation is given in the previous paper [10]. During the growth of rod-shaped precipitates the hardness increases relative slowly (Fig. 1).

An example of the preliminary wide-angle measurements is shown in Fig. 3. According to the 111 reflection, the size of Ge precipitates is about 250 Å, when the specimen was quenched from a temperature of 480°C and aged at 160°C for 3000 min. Side maxima were observed in both the 111 and 311 reflections. The side maximum is located at a smaller  $2\theta$  value than the corresponding main reflection.

The present X-ray and microhardness studies show that the precipitation of germanium in an Al-4.0 wt % Ge alloy depends upon the content of quenched-in vacancies. After quenching, the number of precipitates increases with quenched-in vacancies, while the mean size of the precipitates is independent of the vacancy concentration. If the vacancy concentration is high enough, a short ageing at 160°C reduces the number of Ge precipitates. When ageing of 160°C is prolonged, rod-shaped Ge precipitates are formed. This growth process also depends on the number of quenched-in vacancies.

### Acknowledgement

The grant received from the Finnish State

Committee for Natural Science in support of this study is gratefully acknowledged.

### References

1. M. BELLER and V. GEROLD, *Z. Metallk.* **61** (1970) 659.
2. M. BELLER, *ibid* **63** (1972) 663.
3. *Idem*, *ibid* **64** (1972) 189.
4. *Idem*, *ibid* **64** (1973) 387.
5. M. BELLER, P. FÜRNRÖHR and V. GEROLD, *Phys. Stat. Sol. (a)* **17** (1973) 435.
6. S. CERESARA and P. FIORINI, *Mat. Sci. Eng.* **7** (1971) 168.
7. J. E. EPPERSON, P. FÜRNRÖHR and V. GEROLD, *Acta Met.* **23** (1975) 1381.
8. U. KOESTER, *Mat. Sci. Eng.* **5** (1970) 174.
9. R. I. KUZNETSOVA, V. I. RANYAK and S. Z. FEDORENKO, *Fiz. Metal. Metalov.* **35** (1973) 937.
10. H. KÄHKÖNEN and P. SUHONEN, *J. Mater. Sci.* **10** (1975) 658.
11. L. M. SOROKIN and A. A. SITNIKOVA, *Sov. Phys. Sol. Stat.* **9** (1968) 1525.

Received 15 March

and accepted 3 May 1976

HEIKKI KÄHKÖNEN

VESA VILJANEN

JARMO KULMALA

Department of Physical Sciences,

University of Turku,

SF-20500 Turku 50, Finland

### Fracture morphology of rigid poly(vinyl chloride)

It is clearly indicated that the cracks in many thermoplastics are generated from the prior formation of crazes [1-5]. In the case of poly(vinyl chloride) (PVC), although thermoplastic, the existence of crazes and their role in the fracture process is still enigmatic, because contradictory results have been published concerning the existence of precrack crazes in PVC. For example, Gotham [6] and Cornes and Haward [7] refer to crazing in rigid PVC, but Kambour [8] found no evidence of precrack craze formation. Because the later stages of fracture in PVC are not clearly known we have studied the nucleation and morphology of fracture in rigid PVC under tensile test conditions.

The material, which was a commercial suspension type PVC (K value of 58), was supplied by

Pekema Oy in the form of injection-moulded dumb-bell-shaped test pieces (ASTM D 638). It did not contain plasticizer, but small amounts (< 7 % w/w) of stabilizers and lubricants were added.

Tensile tests were carried out at room temperature ( $23 \pm 1^\circ\text{C}$ ). Tests were performed in simple uni-axial tension using an Instron tensile testing machine (floor model) at constant speeds of 0.5, 1.0 and 5.0 mm min<sup>-1</sup>. The specimens and fracture surfaces were examined using a scanning electron microscope (SEM) (model JEOL JSMU 3), a transmission electron microscope (TEM) (model JEOL 100B) and by light microscopic methods. The SEM samples were coated with carbon and gold. The TEM samples were cast into epoxide polymer and cut using a microtome with a diamond knife (150 to 200 nm thick slices).

When tensile stress was applied to test pieces, stress whitening, necking and extension of the test

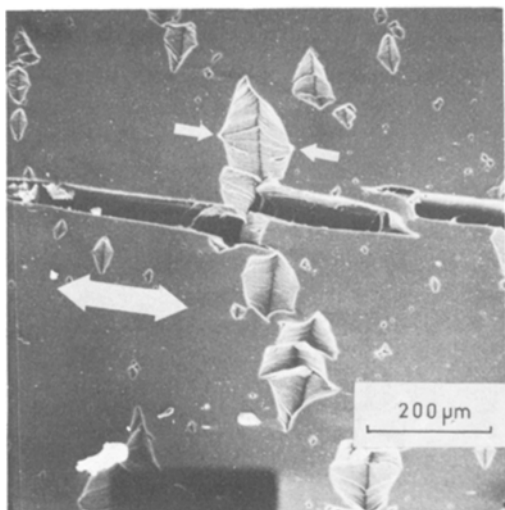


*Figure 1* Scanning electron micrograph of the cavities on the surface of a PVC test piece. The direction of tensile stress is given by the large arrow. The small arrows indicate the remnants of the nucleation centre of one cavity.

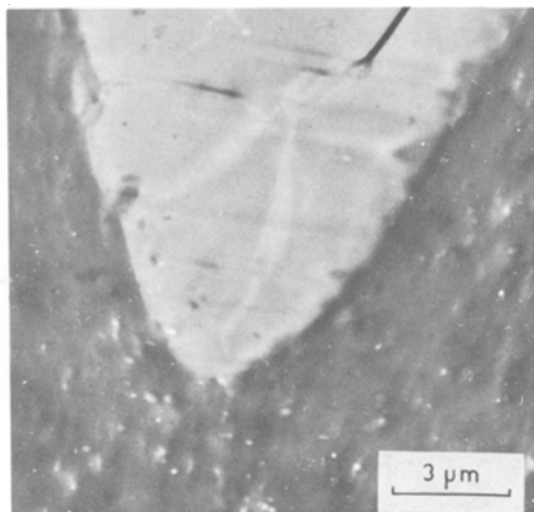


*Figure 2* Transmission electron micrograph of the cross-section of a cavity.

piece took place, followed by a rupture within the necked region of the specimen.

Tension caused the formation of cavities on the broad surfaces of the test pieces (Fig. 1). The cavities were, as a rule, oriented normal to the drawing direction. A crack which is parallel to the tensile axis is also seen in Fig. 1. Some such cracks were formed during the final stage of test piece failure. Evidently this process has some kind of relationship to the fibrous fractures of polymers described by Peterlin [9]. The nucleation of cavities began immediately after the beginning of cold flow (necking). During the propagation of cold flow, the growth of cavities practically ceased. The cavities nucleated on the broad surfaces of test pieces and their growth advanced continuously from the nucleation centre. The tensile test speed in the used region had no effect on either the amount or the morphology of the cavities. No crazes were found by SEM or by light microscopy as precursors of cavities. Neither were crazes observed at the bottom of the cavities (Fig. 2).

The bottoms of the cavities were blunt, (Figs. 2 and 3) and therefore differed clearly from the sharp cracks which grow by propagation into crazes, e.g. in poly(styrene) [1]. Only after several weeks did crazes appear on the surfaces of test

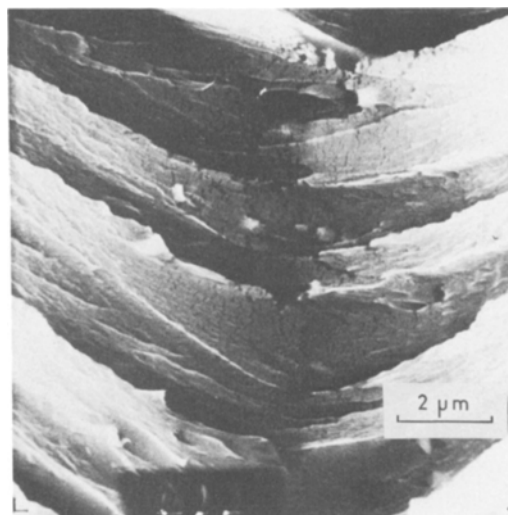


*Figure 3* Scanning electron micrograph of the bottom of a cavity.

pieces. Their direction was normal to the stress axis as reported by Cornes and Haward [7]. However, in our test pieces these crazes were clearly a consequence of environmental stress crazing caused by residue stresses.

The dimensions of the cavities in the test pieces varied considerably: the smallest were  $\sim 3.5 \mu\text{m}$  long and the largest  $\sim 40$  times longer. However, in their morphology they were alike. Evidently

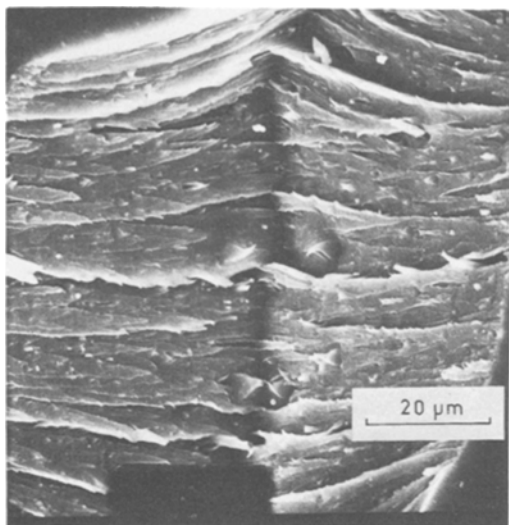


Figure 4 The structure of the walls of a cavity.

cavities nucleate from dot-like stress concentrations on the surface of test piece. The remnants of the nucleation centre are clearly seen as sharp points on both walls of the cavity (small arrows in Fig. 1). Cavities grow by fan-like propagation normal to the drawing direction, and their walls are composed of both large and small strips with wedge-like points. The smaller strips are located on the surfaces of the larger ones (Fig. 4).

The morphology of the cavities markedly resembles that of diamond cavities reported by Cornes and Haward [7]. However, in this case the cavities do not have blunt edges normal to the drawing direction. Figs. 2 and 3 also indicate that the bottom of the cavity is parabola-shaped and

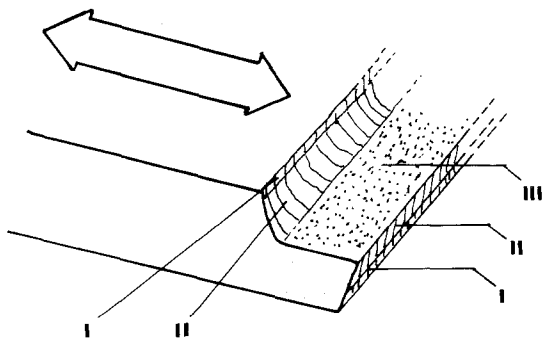


Figure 5 A schematic illustration of the fracture surface of the injection-moulded test piece. The direction of tensile stress is shown by the arrow. The different fracture zones are indicated by numbers I, II and III (cf. text).

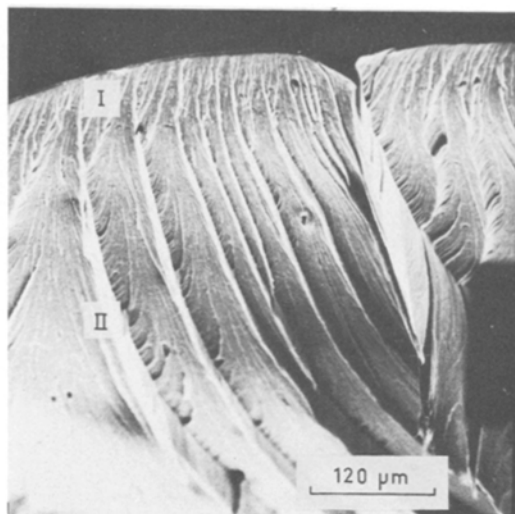


Figure 6 Zones I and II on the fracture surface of a test piece.

that the growth of the cavity advances by ductile tearing of material in the direction parallel to the tensile axis.

The fracture surfaces of test pieces contained five different zones, which are illustrated schematically in Fig. 5.

The catastrophic failure of a test piece is preceded by the growth and coalescence of the cavities. A coherent crack is immediately formed which extends over the surface of test piece (zone I in Figs. 5 and 6). Subsequently, zone II is formed

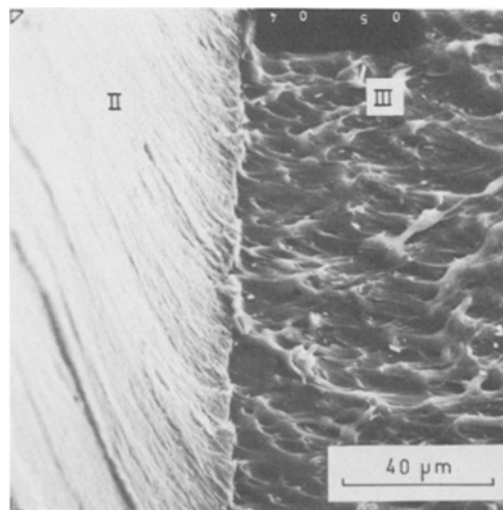


Figure 7 Zones II and III on the fracture surface of a test piece.

when a crack propagates evenly about the centre of the test piece. Zone II is characterized by strong, growing ridges which are oriented to the direction of tensile axis (Fig. 6). In the middle of the test piece, zone II abruptly changes to zone III (Fig. 7). The surface of zone III is macroscopically plain, but the examination of its fine structure reveals that it is scaly and clearly partly melted. Zone III is oriented parallel to the wide surfaces of test piece. Because the remaining zones (I and II on the other side of zone III) have identical structures with the former zones I and II, we conclude that the fracture surface of an injection-moulded test piece is generated by two cracks which propagate similarly from both wide surfaces of the test piece. In the middle of the test piece, the longitudinal stress causes an abrupt crack formation between the bottoms of the cavities. Simultaneously, a considerable amount of heat energy is liberated, which melts the surface of zone III. The existence of fracture zones I, II and III could possibly be explained by means of the different degrees of orientation in different parts of an injection-moulded test piece [10].

### Acknowledgements

The authors thank the Foundation of Neste OY for financial aid and Esko Pääkkönen for technical assistance.

### References

1. P. BEAHAN, M. BEVIS and D. HULL, *Phil. Mag.* **24**

- (1971) 1267.
2. R. P. KAMBOUR, *J. Polymer Sci. Makromol. Rev.* **7** (1973) 1.
3. T. E. BRADY and G. S. Y. YEH, *J. Mater. Sci.* **8** (1973) 1083.
4. T. L. PETERSON, D. G. AST and E. J. KRAMER, *J. Appl. Phys.* **45** (1974) 4220.
5. E. L. THOMAS and S. J. ISRAEL, *J. Mater. Sci.* **10** (1975) 1603.
6. K. V. GOTHAM, *Plast. Polym.* **37** (1969) 309.
7. P. L. CORNES and R. N. HAWARD, *Polymer* **15** (1974) 149.
8. R. P. KAMBOUR, *J. Polymer Sci. (A-2)* **4** (1966) 17.
9. A. PETERLIN, "Polymeric Materials", edited by E. Baer and S. V. Radcliffe (American Society for Metals, Metals Park, 1975) p. 175.
10. T. W. OWEN and D. HULL, *Plast. Polym.* **42** (1974) 19.

Received 23 March  
and accepted 3 May 1976

P. TORMALA  
*Institute of Materials Science,  
Tampere University of Technology  
SF-33101 Tampere 10,  
Finland*

S. LEHTINEN  
J. J. LINDBERG  
*Department of Wood and Polymer Chemistry  
University of Helsinki,  
SF-00100 Helsinki 10,  
Finland*

### *Martensitic transformation cubic $\rightleftharpoons$ rhombohedral in rubidium nitrate*

The degree to which potentially martensitic mechanisms are affected by orientational disorder and atomic mobility is an important aspect of crystal structural transformations [1, 2]. It is also of interest to examine a material which transforms from cubic NaCl-related to an intermediate rhombohedral structure, in order further to clarify details of the large change NaCl type  $\rightarrow$  CsCl type in which the primitive rhombohedral angle alters from  $60^\circ$  to  $90^\circ$  and which was investigated in  $\text{NH}_4\text{Br}$  [3]. Two types of orientation relation were found, close to  $(100)_{\text{NaCl}} \parallel (110)_{\text{CsCl}}$ ,

$[010]_{\text{NaCl}} \parallel [\bar{1}11]_{\text{CsCl}}$  (type A), and  $(100)_{\text{NaCl}} \parallel (100)_{\text{CsCl}}$ ,  $[010]_{\text{NaCl}} \parallel [101]_{\text{CsCl}}$  (type B). Different authors have suggested new lattice correspondences [4, 5]. That of Hyde and O'Keefe [4] however, appears to be equivalent, for MX compounds, to the conventional contraction of  $[111]$ , leading to A type. Further data on B would be appropriate.

Rubidium nitrate provides the fcc parent lattice with marked orientational disorder in phase I [6, 7]; the rhombohedral structure in phase II, below  $284^\circ\text{C}$  [8]; and a CsCl-related cubic form III below  $219^\circ\text{C}$ . Phase III was earlier found to be in an orientation of type B with respect to I when the crystal was slowly cooled through II [9].